Two zinc-binding domains in the transporter AdcA from *Streptococcus pyogenes* facilitate high-affinity binding and fast transport of zinc

Kun Cao[#], Nan Li[#], Hongcui Wang[#], Xin Cao, Jiaojiao He, Bing Zhang, Qing-Yu He[*], Gong Zhang[*], Xuesong Sun[*]

From the Key Laboratory of Functional Protein Research of Guangdong Higher Education Institutes, Institute of Life and Health Engineering, College of Life Science and Technology, Jinan University, Guangzhou 510632, China

Present address: 601 Huang-Pu Avenue West, Guangzhou 510632, China

Running Title: *Two zinc-binding domains in AdcA facilitate zinc transportation*

***Correspondence should be addressed to**: Prof. Xuesong Sun, Tel & Fax: +86-20-85226165, E-mail: tsunxs@jnu.edu.cn; Prof. Qing-Yu He, Tel & Fax: +86-20-85227039, E-mail: tqyhe@jnu.edu.cn; Prof. Gong Zhang, Tel: +86-20-85224031, E-mail: zhanggong@jnu.edu.cn.

SUPPORTING INFORMATION

Table S1. Primer Sequences used in this study.

Primers	Sequence(5′-3′)	Comments
AdcA up	CGCGGATCCACTCAGGCAAAACAAGTCTTAGC	purification
AdcA down	CGCGTCGACTTAATGAGCATTGATTTCTTGGGC	for AdcAs
N-lobe up	ATTGGATCCACTCAGGCAAAACAAGTCTTAGCAG	purification
N-lobe down	ATTGTCGACTTACACATCAGTGGTTAAGCGTAAG	for N-lobes
C-lobe up	CTTGGATCCGCTGGTAAAGAAATTCTTCCAG	purification
C-lobe down	CGCGTCGACTTAATGAGCATTGATTTCTTGG	for C-lobes
H36A	CTTATGAAAGCAGGAACGGAACCTGCTGATTTTGAGCCTTCTAC	
H122A	CACAACCATGCTTTTGACCCAGCCGTGTGGTTGTCAC	sites-directed mutagenesis
H186A	GCAAAAGAGCTTTGTGACACAAGCCGCAGCTTTTGGTTATATG	for C-AdcA
E261A	CTGTGCTTAGTCCGCTTGCAGGTTTGACTGAAAAAGA	
H436A	AAATACGTTCAATTCAGTGACGCTGCCATTGCTCCTGAAAAAGC	
H445A	GCTCCTGAAAAAGCAAAGGCTTTCCACCTGTACTGGGG	sites-directed mutagenesis
H447A-1	TGAAAAAGCAAAGCATTTCGCCCTGTACTGGGGTGGTGAC	for N-AdcA
H447A-2	GCTCCTGAAAAAGCAAAGGCTTTCGCCCTGTACTGGGG	
P1-*AdcA*	GCCATAGTTAGGGGCTTT	
P2-*AdcA*	GTCATGAGCAAGGGTAAA	gene knockout
P3-*AdcA*	ATCAAACAAATTTTGGGCCCGGTGAGAAATCGACTAGTTC	for *adcA*
P4-*AdcA*	ATTCTATGAGTCGCTGCCGACTGTTCGTCTCCTATTTGAT	
P1-*AdcAII*	CCCTATCGCGTATGATTT	
P2-*AdcAII*	TCCTTGGGCTCTGGCTGC	gene knockout

P3-*AdcAII*	CTAAATTTTTATCTAAAGTGAATTTGAACAACTCCTTAACCAT	for *adcAII*
P4-*AdcAII*	CCTTAACAATCCCAAAACTTGTCGAGGAAAGAATGAAAATCAA	
p169-*N-lobe* up	ACGGGGCCGGAGACCGCGGTATCGTGACAACCTTTTACCCTGTCT	overexpression for *p169-N-lobe*
p169-*N-lobe* down	CGGGTACCGAGCTCCCGCGGTTTAGTGATGGTGATGGTGATGT CCTCTGCCTTTTCAGG	
p169-*C-lobe* up	ACGGGGCCGGAGACCGCGGTTACCAAGACAGTCCAAAA	overexpression for *p169-C-lobe*
p169-*C-lobe* down	CGGGTACCGAGCTCGAATTCTCAGTGATGGTGATGGTGATGA TGCGCCAACATTTC	
p169-*adcA* up	ACGGGGCCGGAGACCGCGGTATCGTGACAACCTTTTACCCTGTCT	overexpression
p169-*adcA* down	CGGGTACCGAGCTCCCGCGGTTCAGTGATGGTGATGGTGATG ATGCGCCAACATTTC	for *p169-adcA*

Table S2. The Secondary Structural Contents of apo-AdcA and Zn_2-AdcA.

Secondary structure (%)	*Helix*	*Strand*	*Turn*	*Unordered*
apo-AdcA	53.2 ± 0.62	18.5 ± 0.29	8.6 ± 0.11	19.1 ± 0.14
Zn_2-AdcA	58.8 ± 0.14	19.4 ± 0.24	11.3 ± 0.29	11.2 ± 0.56

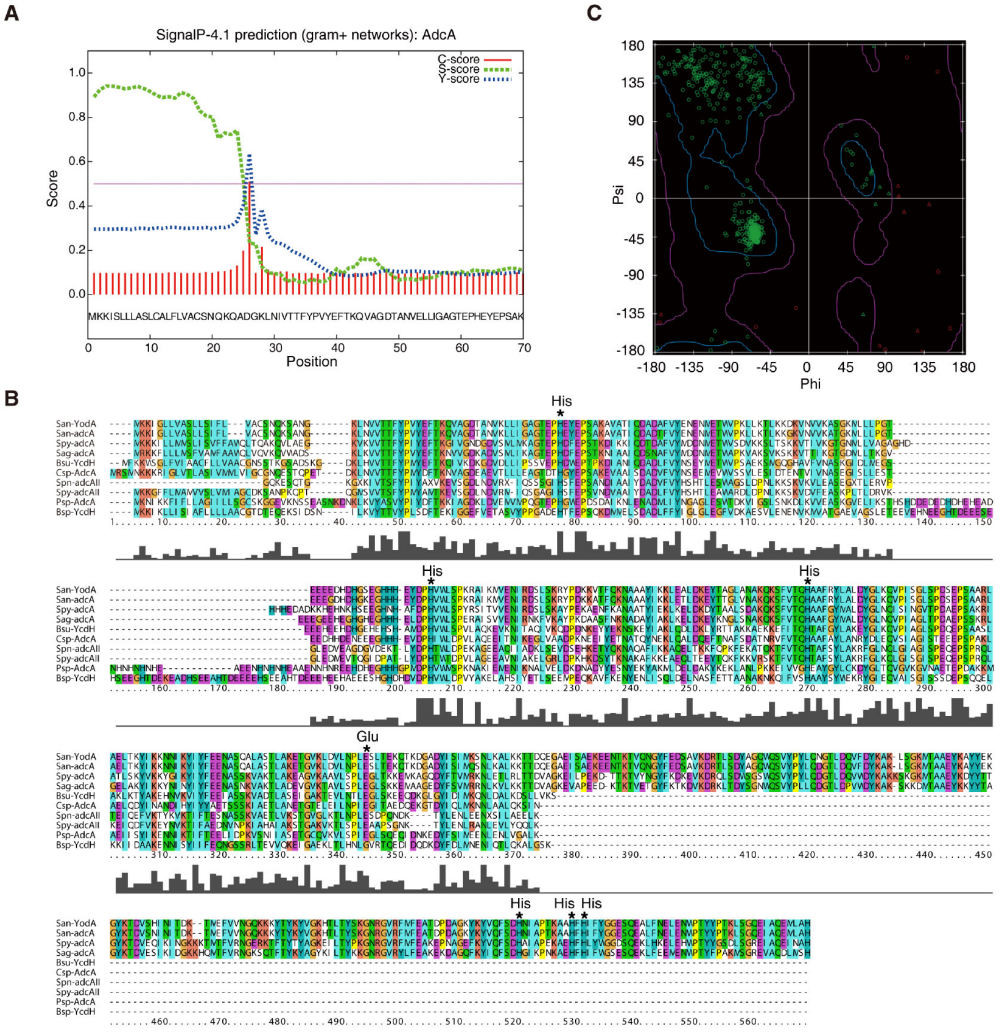

Fig. S1 Bioinformatic analysis of AdcA. (A) Prediction of the signal peptide of AdcA by SignalP-4.1 Server (green line). (B) Sequence alignment of AdcA with homologous proteins (*San*-YodA, *San*-AdcA, *Sag*-AdcA, *Bsu*-YcdH, *Csp*-AdcA, *Spn*-adcA II, *Spy*-adcA II, *Psp*-AdcA, and *Sp*-YcdH) using the Clustal-X software program with tinting depending on the properties of the amino acids. The predicted zinc-binding sites are marked above the aligned sequences. (C) The Ramachandran plot of the AdcA structure modeled via homology. 93.3% of the modeled AdcA residues are in the acceptable regions (blue). The purple region denotes the "marginal region".

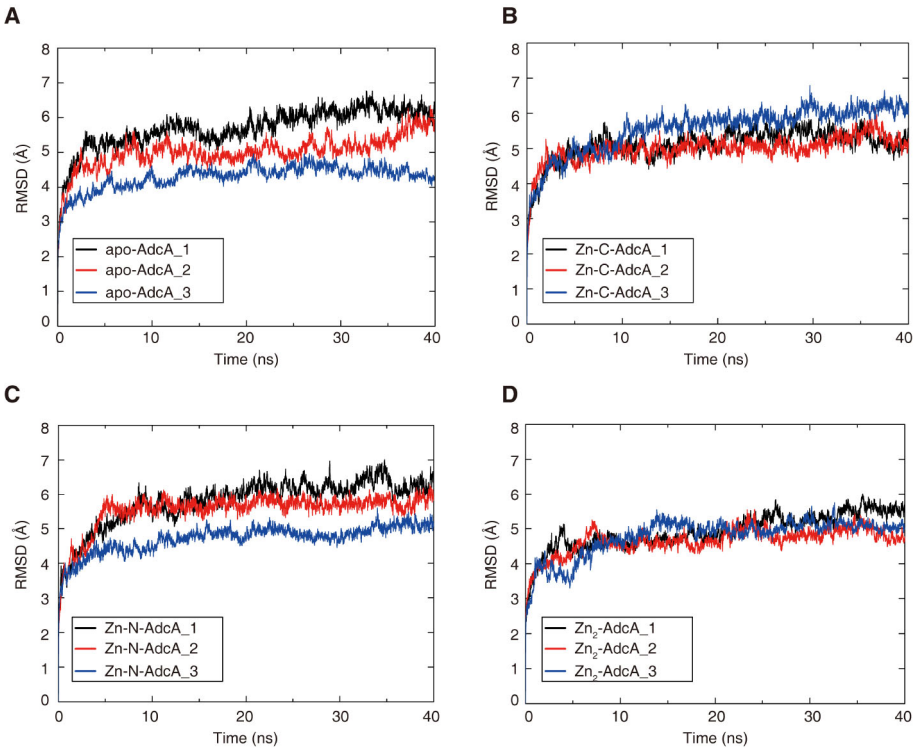

Fig. S2 Three simulation repeats based on different initial velocities. The four structural models of apo-AdcA (A), Zn-C-AdcA (B), Zn-N-AdcA (C), and Zn_2-AdcA (D), with different treatments, were analyzed using the MD simulation system.

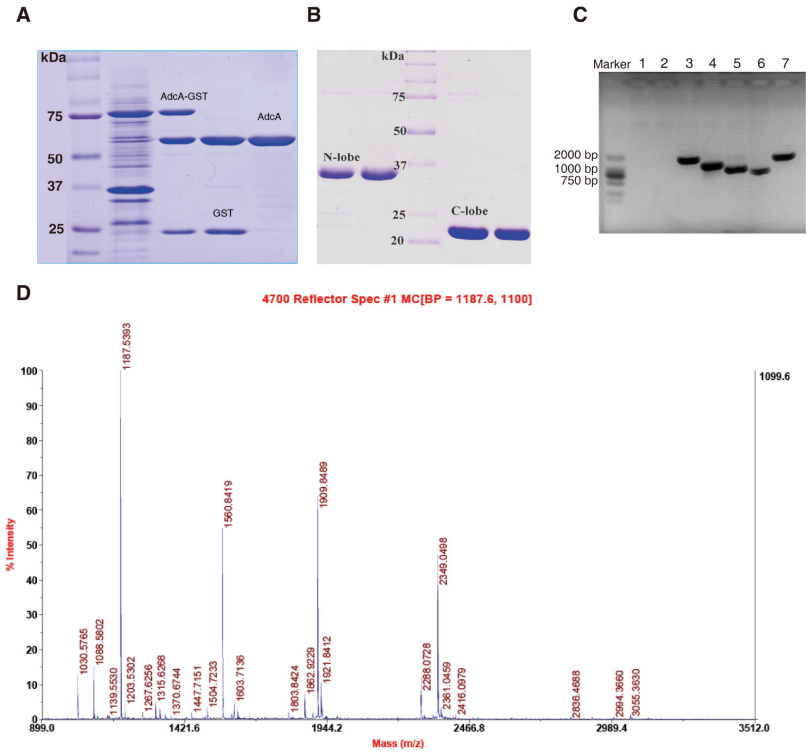

Fig. S3 Protein expression and confirmation. Protein purity of apo-AdcA (A) N-lobe and C-lobe (B) detected by 12% SDS-PAGE gel. (C) PCR detection of *adcA* (lane 1) and *adcAII* gene (lane 2) in the *ΔadcAΔadcAII* double-mutant strains, the molecular weight of *adcA* and *adcAII* (lane 3 and 4), genes encoding *N-lobe* (lane5), *C-lobe* (lane 6), and *adcA* (lane 7) in overexpression strains. (D) MS spectrum of AdcA detected using mass spectroscopy (ABI 4800 MALDI-TOF/TOF).

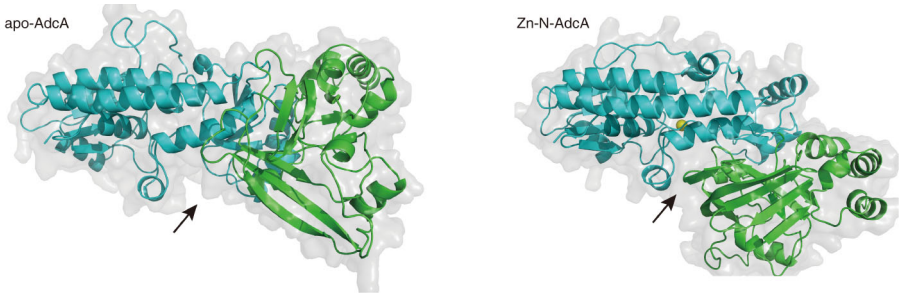

Fig. S4 Representative surface structures of apo-AdcA and Zn-N-AdcA after 90° of rotation of Figure 5. The adjacent inter-domain surface formed, between the N-terminal domain and C-terminal domain, is indicated by an arrow.

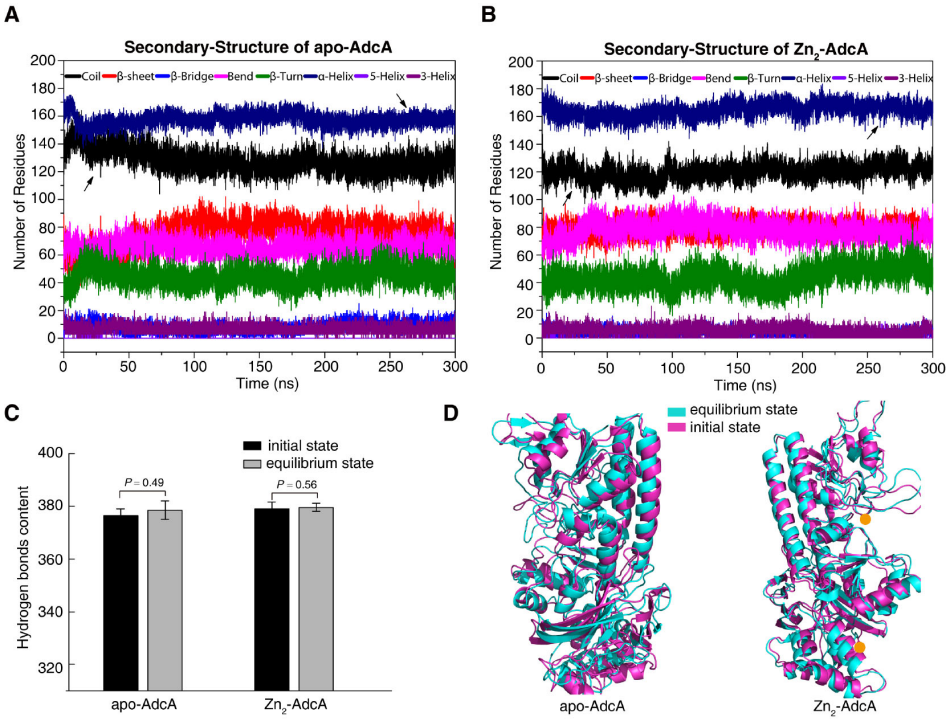

Fig. S5 Structure of apo-AdcA and Zn_2-AdcA in a 300-ns MD simulation. The numbers of residues involved in various secondary structures are shown in detail: coil, β-sheet, β-bridge, bend, β-turn, α-helix, 5-helix, and 3-helix. These structures of apo-AdcA (A) or Zn_2-AdcA (B) were calculated over the 300-ns simulation. (C) Hydrogen bonds in the initial and equilibrium states of the two proteins. (D) Comparison of the average conformation of the equilibrium and initial states.

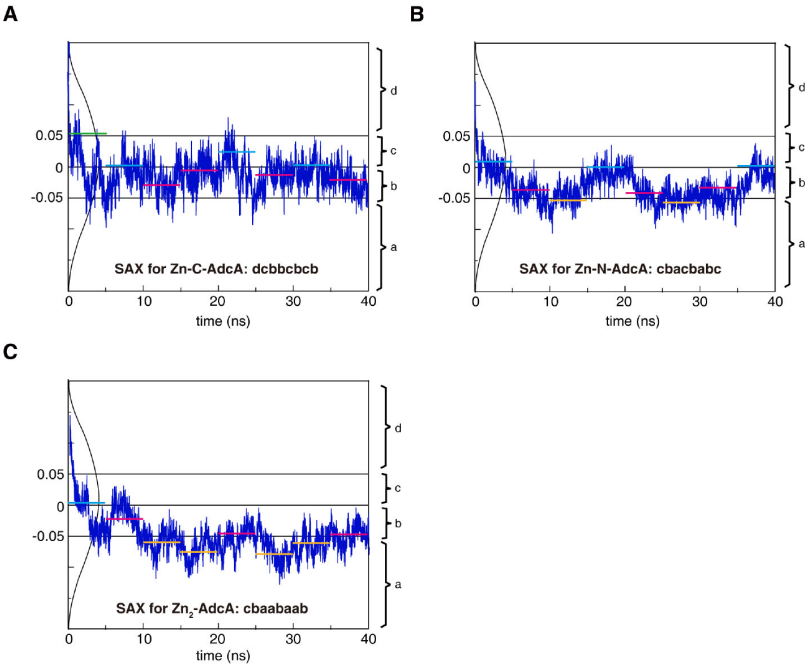

Fig. S6 Comparison of three curves of Zn-C-AdcA, Zn-N-AdcA, and Zn_2-AdcA in Fig. 2F

using the SAX method. The discretization of the time series, with lengths of 40 ns, are mapped to three different strings. We converted the curve to an eight-symbol string (alphabet of size 4, A = 5) and corresponding values are shown in the diagrams: Zn-C-AdcA (A), Zn-N-AdcA (B), and Zn_2-AdcA (C).

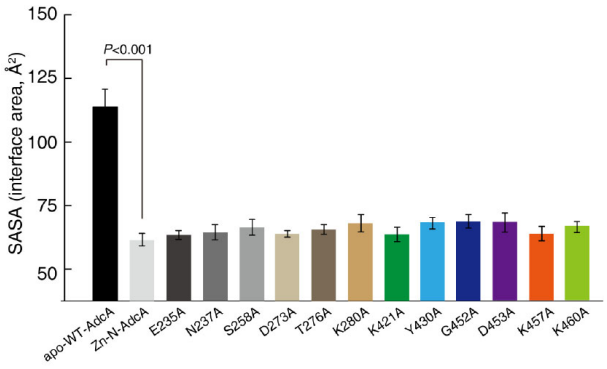

Fig. S7 SASA of WT and single-point mutant Zn-N-AdcA.

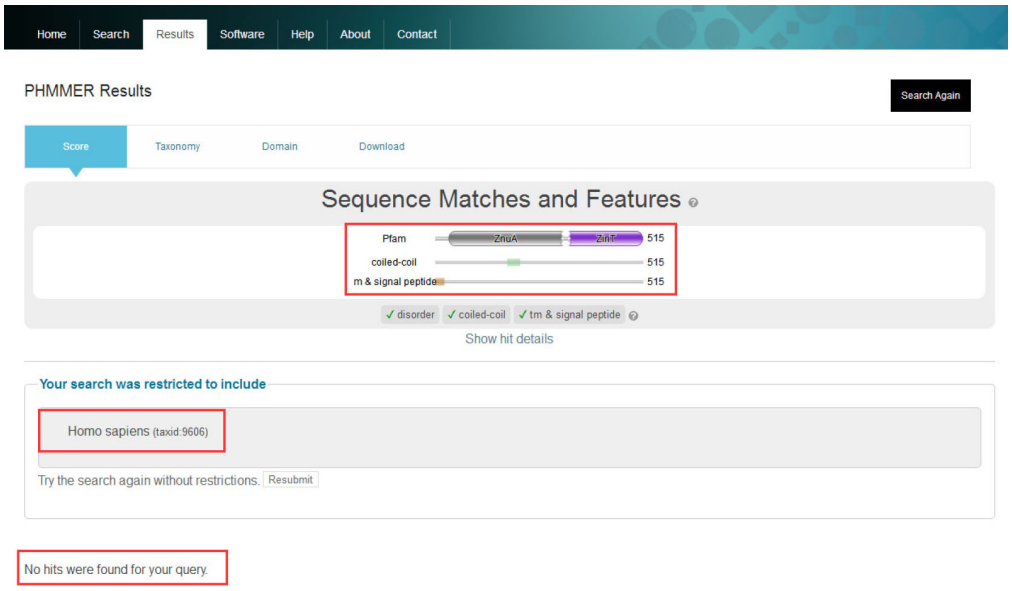

Fig. S8 Comparison of AdcA sequence to the database of Ensemble Human using HMMER program.